EUKARYOTIC CELL, July 2008, p. 1098–1108 Vol. 7, No. 7
1535-9778/08/$08.00+0 doi:10.1128/EC.00109-07


# Functional Characterization of CgCTR2, a Putative Vacuole Copper Transporter That Is Involved in Germination and Pathogenicity in *Colletotrichum gloeosporioides*▽†

Sima Barhoom,[1] Martin Kupiec,[2] Xinhua Zhao,[3] Jin-Rong Xu,[3] and Amir Sharon[1]*

*Department of Plant Sciences, Tel Aviv University, Tel Aviv 69978, Israel[1]; Department of Microbiology and Biotechnology, Tel Aviv University, Tel Aviv 69978, Israel[2]; and Department of Botany and Plant Pathology, Purdue University, West Lafayette, Indiana 47907[3]*

Received 5 April 2007/Accepted 10 April 2008

**Copper is a cofactor and transition metal involved in redox reactions that are essential in all eukaryotes. Here, we report that a vacuolar copper transporter that is highly expressed in resting spores is involved in germination and pathogenicity in the plant pathogen *Colletotrichum gloeosporioides*. A screen of *C. gloeosporioides* transformants obtained by means of a promoterless green fluorescent protein (GFP) construct led to the identification of transformant N159 in which GFP signal was observed in spores. The transforming vector was inserted 70 bp upstream of a putative gene with homology to the *Saccharomyces cerevisiae* vacuolar copper transporter gene *CTR2*. The *C. gloeosporioides CTR2* (Cg*CTR2*) gene fully complemented growth defects of yeast *ctr2*Δ mutants, and a CgCTR2-cyan fluorescent protein (CFP) fusion protein accumulated in vacuole membranes, confirming the function of the protein as a vacuolar copper transporter. Expression analysis indicated that Cg*CTR2* transcript is abundant in resting conidia and during germination in rich medium and downregulated during "pathogenic" germination and the early stages of plant infection. Cg*CTR2* overexpression and silencing mutants were generated and characterized. The Cg*ctr2* mutants had markedly reduced Cu superoxide dismutase (SOD) activity, suggesting that CgCTR2 is important in providing copper to copper-dependent cytosolic activities. The Cg*ctr2*-silenced mutants had increased sensitivity to $H_2O_2$ and reduced germination rates. The mutants were also less virulent to plants, but they did not display any defects in appressorium formation and penetration efficiency. An external copper supply compensated for the hypersensitivity to $H_2O_2$ but not for the germination and pathogenicity defects of the mutants. Similarly, overexpression of Cg*CTR2* enhanced resistance to $H_2O_2$ but had no effect on germination or pathogenicity. Our results show that copper is necessary for optimal germination and pathogenicity and that CgCTR2 is involved in regulating cellular copper balance during these processes.**

Spores of plant-pathogenic fungi can germinate in water, unlike spores of "saprophytic" species, which usually germinate in the presence of sugars (8, 17). In many cases germination is stimulated by specific plant compounds or by physicochemical properties of the supporting surface. In *Colletotrichum* species cuticular waxes or plant volatiles can induce germination (19, 26). Spore germination in soil-borne fungi is enhanced by root exudates, while in rust fungi spores are sensitive to the leaf surface properties (2, 12). Hard hydrophobic surfaces can replace plant-derived signals and are sufficient to trigger spore germination in several species, including *Magnaporthe grisea*, *Botrytis cinerea*, and *Colletotrichum* species (7, 8, 11, 15).

Spore germination is regulated by different signaling cascades. In most species heterotrimeric G proteins, cyclic AMP (cAMP), and mitogen-activated protein (MAP) kinase cascades are involved in the activation of germination as well as in the regulation of specific developmental stages during germination. In *Colletotrichum lagenarium* germination is controlled by at least two signaling cascades, a cAMP-dependent pathway and the CMK1 MAP kinase (homolog of *M. grisea* PMK1) pathway (29). Additional signaling elements might be involved, e.g., primarily calcium-dependent signals and other MAP kinase pathways (11, 13, 27). Germination in the gray mold fungus *B. cinerea* is regulated by at least three signaling pathways, which include a Gα protein BCG3, a cAMP pathway, and the FUS3/PMK1 MAP kinase homolog BMP1 (8). Each of these pathways mediates germination in response to different signals including carbon source, surface hardness and hydrophobicity, or specific nutrients. Spore germination in *M. grisea* does not require the PMK1 or Gα/cAMP pathways; however, these pathways regulate the following formation of appressoria, which are specialized organs that differentiate at the end of germ tubes and are used for plant penetration (31, 33). Moreover, 19 out of 67 genes that were highly expressed in appressoria compared to mycelium also showed high levels in dormant spores (30). Thus, in plant-pathogenic fungi, spore germination and early pathogenic development are tightly linked and are regulated by common signaling pathways.

*Colletotrichum gloeosporioides* f. sp. *aeschynomene* is a hemibiotrophic plant pathogen that specifically attacks the weed *Aeschynomene virginica*. The fungus produces large numbers of asexual spores that, following a contact with plant organs, germinate, form appressoria, and penetrate the plant. We pre-

* Corresponding author. Mailing address: Department of Plant Sciences, Tel Aviv University, Tel Aviv 69978, Israel. Phone: 972 3 640 6741. Fax: 972 3 640 5498. E-mail: amirsh@ex.tau.ac.il.

† Supplemental material for this article may be found at http://ec.asm.org/.

▽ Published ahead of print on 2 May 2008.

viously showed that *C. gloeosporioides* can germinate in two distinct ways: "pathogenic" and "saprophytic" (3). Pathogenic germination takes place on plants or on a hydrophobic surface and is characterized by fast mitosis followed by development of a single germ tube. The process is initiated immediately following induction and terminates within 4 h with the formation of appressoria. Saprophytic germination occurs in rich medium; it takes a much longer period of time and is characterized by development of two germ tubes that emerge from opposite sides of the spore. These germ tubes do not form appressoria, and therefore spores that germinate in this way do not infect plants. The two germination styles in *C. gloeosporioides* are regulated by different signaling cascades; saprophytic germination is enhanced by cAMP while pathogenic germination is cAMP independent, but, similar to *M. grisea*, cAMP is required later for appressorium formation (3). The association between germination style and the subsequent pathogenic development suggests that genes that are necessary for pathogenic spore germination may also affect fungal pathogenicity.

To identify genes that are associated with pathogenic germination, we generated a *C. gloeosporioides* promoter-trapping mutant collection by restriction enzyme-mediated transformation (REMI), using the green fluorescent protein (GFP) as a reporter for gene expression. We screened this collection for transformants that had specific GFP expression patterns under saprophytic and pathogenic germination conditions. Here, we report on the characterization of a REMI mutant in which GFP expression was enhanced in spores and suppressed during pathogenic germination. The tagged locus was isolated and found to encode a putative vacuolar copper transporter that has not been previously characterized in filamentous fungi. Functional analysis of this gene revealed that it is involved in resistance to oxidative stress, but it does not affect sensitivity to copper. We also found that this gene is necessary for pathogenic germination as well as for full virulence but not for saprophytic germination. These results suggest that copper is necessary for proper germination and pathogenesis in this fungus.

## MATERIALS AND METHODS

**Fungi and plants.** *C. gloeosporioides* f. sp. *aeschynomene* strain 3.1.3 and transgenic strains were used. Emerson's YPSS (EMS), pea extract (PE), regeneration (REG) and Czapek-Dox (CD) solid and liquid media were prepared as previously described (25). Pathogenicity tests were performed on 12-day-old *Aeschynomene virginica* plants or on the first true leaves of *Pisum aestivum* cv. white sugar (3). *M. grisea* wild-type strain 70-15 and transgenic strains were cultured on oatmeal agar plates at 25°C under fluorescent light (32).

**Generation of REMI collection.** Plasmid pAS1 (provided by W. Schäfer) was digested with NcoI and SphI and the *EGFP* (where EGFP is enhanced green fluorescent protein) coding sequence was cloned between NcoI and SphI sites in place of the luciferase gene to produce the plasmid pAS-GFP. *C. gloeosporioides* was transformed by electroporation of spores (26) with 1 μg of NcoI-linearized pAS-GFP.

**Isolation and sequencing of *C. gloeosporioides CTR2* (Cg*CTR2*).** Genomic regions flanking the inserted pAS-GFP cassette were isolated by inverse PCR (Expand Long Template PCR System; Boehringer) using GFP-specific primers. Additional sequences were isolated by genome walking (Universal Genome Walker Kit; Clontech) using the primers (5′ to 3′) 159pbcl-for (TGTCGTGAT CACTTGAGTCGCGGACC) and 159end-new (GGGGGAGCTCTTTCAATG GCAGGCG). Full-length cDNA sequences were obtained by reverse transcription-PCR ([RT-PCR] Reverse-iT 1st Strand Synthesis Kit; ABgene) with primers 159end-new and 159-start (GAAATTTCCGCGTCATAATGGACCACG) and by rapid amplification of cDNA ends ([RACE] 5′/3′ RACE kit; Roche) using primers 5race159-rev (ATTACTTGCGCTTGTTCGGGGGG) and 5race159-nr (AAACTGTTGGCAACAGCTCCCCGCC).

**Construction of plasmid vectors. (i) Ksh-CgCTRi: Cg*CTR2* silencing vector.** Fragments from bp 1 to 700 and 1 to 1024 of the Cg*CTR2* genomic sequence were amplified by PCR using the primer pair Dw-1Bmfor (CCACAGGATCC ATGGGCGGCCACGGCGGTA) and Up-716sp (GTCTCAGTACTAGTGCC AGCGATGCC) and the pair Up-1Ncfor (CCACAAGCACCATGGGCGGCC ACGG) and Dw-1024sp (CCCAGCACTAGTAAGTCATAAAGATAAGC). The 1,024-bp fragment was cloned into NcoI/SpeI sites of pGEMT (Promega). The 700-bp fragment was cloned into SacI and SpeI sites of the resulting plasmid. The two fragments in opposite orientations were released by digestion with NcoI and BamHI and cloned between the *GPDA* promoter and *TRPC* terminator in pKsh52-1 (4).

**(ii) Ksh-CgCTR: Cg*CTR2* overexpression vector.** The full-length Cg*CTR2* genomic clone (1.2 kb; accession number EF434817) was amplified by PCR with the primers 159oe-Bsph (GAAATTTCCGCGTCATCATGAACCACG) and 159oe-Bgl (GAATGGGGGAGATCTTTCAATGGCAGGCGTTG) and cloned into BspHI and BglII between the *GPDA* promoter and *TRPC* terminator in pKsh52-1.

**(iii) p57-fcgCTR: CgCTR2 complementation vector.** A 3-kb genomic fragment including the Cg*CTR2* promoter (1.8 kb) and open reading frame (ORF; 1.2 kb) was amplified by PCR using the primers 159oe-Bgl (see Ksh-CgCTR) and 159pbcl-for (TGTCGTGATCACTTGAGTCGCGGACC). The fragment was cloned into pTZ57R/T (Ferments).

**(iv) pGMT10-CgCTR2l/s: CgCTR2 yeast expression vector.** The two Cg*CTR2* transcripts (549-bp fragment, accession number EF468351; and 504-bp fragment, accession number EF468352) were amplified by RT-PCR using the primers 159Bm-for (CCGGATCCTAATGGACCACGCACAC) and 159Kpn-rev (CGA TTGGGTACCTCTTTCAATGGCAGGC). The resulting cDNAs were cloned into BamHI and KpnI sites under the *GAL* promoter in pGMT-10.

**(v) CgCTR2-CFP.** Cg*CTR2* cDNA was amplified with primers 159oe-Bsph I (see Ksh-CgCTR) and CTRfusion-Bsph I (GGGGGTCATGATTGAATGGCA GGC) and cloned into an NcoI site on KshCFP (where CFP is cyan fluorescent protein), in frame with the coding sequence of the *CFP* gene, resulting in a fusion protein of CgCTR-2-CFP.

**(vi) pHZ107: Mg*CTR2* complementation vector.** The full-length *M. grisea CTR2* (Mg*CTR2*; BROAD accession no. MG00548) gene was amplified with primers CTRPF (AATAGCGGCCGCAGGACCAGGTATTTGAGTGAATA) and CTRPR (ATAAAAGCTTCATACCTAGATGCTTTGTCATGAT) and cloned into the NotI and HindIII sites on pYK11, which has a bleomycin resistance cassette (33).

**Yeast complementation assay.** *ctr1*Δ, *ctr2*Δ, and *ctr3*Δ yeast cells were transformed with the plasmids pRS416, pRS416-yCTR2, pGMT10-CgCTR2S, and pGMT10-CgCTR2L. Two transformants from each transformation were selected and grown to exponential phase in medium without uracil. Cells were collected by centrifugation, washed with sterile distilled water, and diluted with water to an optical density at 600 nm of 1. Serial dilutions were spotted on selective medium (yeast extract and peptone with 2% ethanol and 3% glycerol [YEPG]) and on YPEG medium with 10, 15, 20, 25, 50, and 100 μM $CuCl_2$. Plates were incubated at 30°C for 3 to 7 days.

**Cg*CTR2* localization.** Transgenic isolates expressing the CgCTR2-CFP fusion cassette were examined using a laser scanning confocal microscope (Zeiss CLSM 510). Staining with FM4-64 and DMY-64 (Molecular Probes) was performed according to the manufacturer's instructions.

**Superoxide dismutase (SOD) activity assay.** Fungi were cultured in CD medium for 48 h, and then the mycelium was harvested. Dry lyophilized mycelia were crushed to powder and suspended in lysis buffer (25 mM Tris-HCl, pH 7.5, 150 mM NaCl, 1 mM EDTA). The samples were centrifuged at 4°C at maximum speed for 10 min. The supernatant was then transferred into new tubes, and the protein concentration was determined. Protein samples (10 μg) were separated on a 12.5% nondenaturing polyacrylamide gel. Gels were incubated for 30 min in the dark in 40 ml of reaction mixture containing 0.1 M potassium phosphate buffer, pH 7.8, 1 mM EDTA, 33 μM riboflavin (Sigma-Aldrich), 245 μM nitroblue tetrazolium (Sigma-Aldrich), and 17 mM TEMED (*N*,*N*,*N*′,*N*″-tetramethylethylenediamine). The gels were then incubated in 0.1 M potassium phosphate buffer, pH 7.8, and 1 mM EDTA and exposed to light for 15 min.

**Mg*CTR2* gene replacement mutants.** Fragments (0.6 kb) upstream and downstream of the Mg*CTR2* coding sequence were amplified with the primer pair CTR1F (CTTGTACGAATACCTACCCAGCAAGTCAT) and CTR2R (AAT AGGCCGGCCGTCGTGATCAGGTTCGTGT) and the pair CTR3F (ATAA GGCGCGCCCTACCTGACCGATCAGGT) and CTR4R (GAGGAGCCCGA GTTTGAGCACAATGAGGATTAT), respectively. The resulting PCR products were digested with FseI and AscI and ligated with the *HPH* (hygromycin B

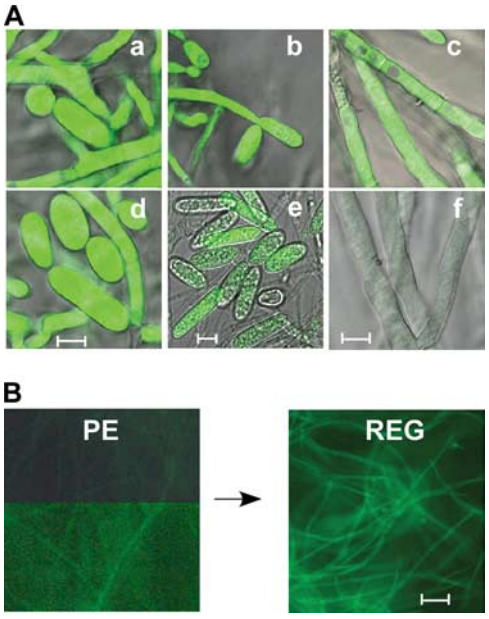


FIG. 1. GFP expression in REMI mutant N159. (A) Strain N159 (bottom) was grown in different media, and GFP signal was compared with a strain expressing GFP from the constitutive *GPDA* promoter (top). The following media were used: REG medium (frames a and d), EMS medium (frames b and e), and PE medium (frames c and f). Scale bar, 5 μm. (B) The GFP signal in strain N159 is reduced in PE medium and recovered in REG medium. The addition of copper and EGTA (a copper chelator) did not affect GFP levels. Contrast and brightness of the lower part of the left picture (PE medium) were intensified to allow visualization of the very low level of GFP expression under these conditions. Scale bar, 30 μm.

phosphotransferase) cassette. The Mg*CTR2* gene replacement construct was amplified with primers CTR1F and CTR4R using the ligation product as the template and directly transformed into *M. grisea* strain 70-15. Hygromycin-resistant colonies were screened by PCR with primers CTRNF (CCAGAGGAGCT GAGCTGT) and CTRNR (ACAGCAAGCATAACCCAA), and strains containing the deletion were confirmed by Southern blot analysis.

**Microscopy.** Fluorescent and light microscopy were performed with a Zeiss Axioskp 2 epifluorescent microscope or with an Olympus SZX 12 fluorescent stereoscope equipped with an EGFP filter. Confocal microscopy was performed with a Zeiss CLSM 510 laser scanning confocal microscope.

**Germination and plant infection assays.** Spores harvested from 5-day-old EMS plates were used to inoculate PE liquid medium. Germination assays were performed in shake cultures or on glass slides (3). Infection assays of *A. virginica* plants and detached pea leaves were performed as previously described (3).

**Mycelium growth.** Radial growth was measured after 5 days of growth on CD or REG agar plates. Media were amended with $CuCl_2$ and or $H_2O_2$.

**Gene expression.** Total RNA was extracted from ground mycelium or germinated spores using a GenElute Mammalian Total RNA Miniprep kit (Sigma) and analyzed by Northern blot hybridization. For semiquantitative RT-PCR, cDNA was generated from 1 μg of RNA using a Reverse-iT 1st Strand Synthesis Kit (ABgene). PCR with Cg*CTR2*-specific primers (159-start and 159end-new) was performed using 4 μl of cDNA as a template. Cg*CDC42*-specific primers (ATGGTCGTCGCTACTATCAAGTGC and TC AGAGGACGAGGCACTTGTGCG) were used as internal controls. The reaction was terminated after 15, 20, 25, 30, 35, and 40 cycles, and amplification products were analyzed by agarose gels. For in planta expression, total RNA was extracted from inoculated pea leaves with an SV Total RNA isolation system (Promega). cDNA was produced with SuperScript II reverse transcriptase (Invitrogen) and the anchored oligo$(dT)_{12–18}$ (Amersham) using 2 μg of RNA as a template. Semiquantitative PCR was performed with 2 μl of cDNA as a template.

**Nucleotide sequence accession numbers.** The three Cg*CTR2* sequences were submitted to GenBank under accession numbers EF434817, EF468351, and EF468352.

## RESULTS

**Characterization of REMI mutant N159.** *C. gloeosporioides* strain 3.1.3 was transformed with the NcoI-digested plasmid pAS-GFP, which includes a promoterless *EGFP* gene adjacent to the NcoI restriction site. Spatial and temporal GFP expression patterns were determined in individual strains that were randomly chosen from more than 4,000 transformants in the REMI collection. In strain N159 bright GFP expression was observed in spores on EMS plates. Further characterization of strain N159 revealed differences in GFP expression under several growth conditions. An intense GFP signal was detected in all organs on high-osmotic medium (REG), whereas on EMS medium the GFP signal was strong in spores and weak in hyphae (Fig. 1A). The GFP signal was hardly detected when the fungus was grown in PE medium and was recovered when the mycelium was transferred from PE to REG medium (Fig. 1B), suggesting that the *EGFP* gene was specifically downregulated in PE medium. The N159 strain had normal morphology on agar plates but had reduced germination compared to the wild-type strain. In a typical assay on glass slides 50% (± 8%) of N159 spores germinated after 2.5 h, compared with 87% (± 4%) germination in the wild-type 3.1.3 strain (Table 1).

**Isolation of the tagged locus in strain N159.** Southern blot analyses confirmed a single insertion of the transformation vector in N159 (data not shown). DNA fragments flanking the insertion site were recovered by inverse PCR, and additional DNA sequences were generated by genome walking. Analysis of the isolated DNA sequence revealed that the pAS-GFP vector was inserted 70 bp upstream of a putative ORF (Fig. 2). Generation of cDNA with primers corresponding to the 5′ and the 3′ ends of the putative ORF yielded two DNA fragments corresponding to 504-bp and 549-bp transcripts. RT-PCR with a primer corresponding to the 3′ end of the gene and a primer matching the 45-bp region that was found only on the larger transcript yielded a single fragment, confirming that both transcripts are encoded by this locus. Comparison of the genomic and cDNA sequences showed that the gene has three introns and that the difference between the two cDNAs is in the third exon (Fig. 2). A BLASTP search with both predicted proteins (183 amino acids [aa] and 168 aa) as a query showed significant similarity to a putative copper transporter from *Candida albi-*

TABLE 1. Spore germination in Cg*CTR2* transgenic strains

| Strain[a] | % Germination (± SD)[b] |
|---|---|
| 3.1.3 (wild type) | 87 ± 4 |
| N159 | 50 ± 8 |
| RNAi 9 | 45 ± 3 |
| RNAi 49 | 42 ± 5 |
| OX35 | 85 ± 3 |
| OX29 | 83 ± 6 |
| C10 | 88 ± 2 |
| C21 | 89 ± 2 |

[a] OX35 and OX29 are Cg*CTR2* overexpression strains. C10 and C21 are Cg*CTR2* complementation strains.

[b] Results are the percentage of spores ($10^6$conidia/ml) that germinated after 2.5 h.

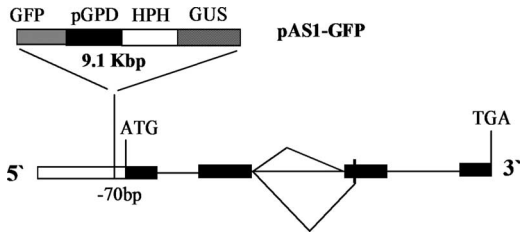


FIG. 2. Schematic diagram of the genomic sequence at the insertion site in strain N159. The insertion site of the transforming vector pAS1-GFP is 70 bp upstream from the start codon of a putative reading frame. Two transcripts are encoded with alternative splicing at 741 bp and 786 bp, corresponding to putative peptides of 183 aa and 168 aa, respectively. Both transcripts have the same reading frame at the 3′ end. Black bars are exons; lines are introns. Positions of the protein transmembrane domains are predicted to be between aa 32 to 54 and 146 to 169 in the larger peptide and between aa 32 to 54, 109 to 132, and 136 to 159 in the smaller peptide. GUS, glucuronidase; HPH, hygromycin B phosphotransferase.

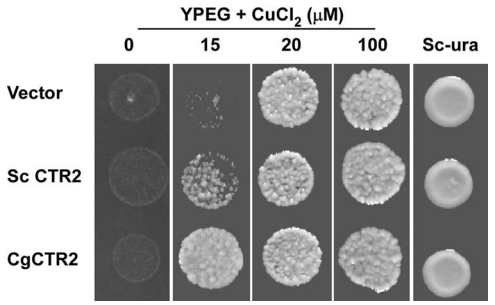


FIG. 3. Complementation of *S. cerevisiae ctr*Δ mutants with Cg*CTR2*. An *S. cerevisiae ctr1*Δ*ctr2*Δ*ctr3*Δ triple mutant was transformed with the *S. cerevisiae CTR2* gene or with Cg*CTR2*. Strains were grown on ethanol-glycerol medium (YPEG) with various concentrations of copper. The triple mutant lacking all three copper transporters requires at least 20 μM $CuCl_2$ for growth on this medium (vector). Transformation of the triple *ctr* mutant with *S. cerevisiae CTR2* (Sc CTR2) restores the ability of the strains to grow on YPEG medium with only 15 μM $CuCl_2$. Transformation of the yeast mutant strain with either the long or short Cg*CTR2* gene fully restored the ability of the complemented strains to grow on medium with 15 μM $CuCl_2$ (CgCTR2). Both transcripts had an identical effect (the result with the long transcript is presented). Growth of the various mutants on synthetic medium (Sc-ura) was unaffected.

*cans* (40% identity) and to *Saccharomyces cerevisiae* Ctr2p (33% identity), a copper transporter of the vacuolar membrane (23). Based on this similarity, we named the gene Cg*CTR2*. Genome searches revealed a single predicted protein with significant homology to CgCTR2 in each of the filamentous fungi for which a genome sequence is available (see Fig. S1 in the supplemental material). Copper transporters are characterized by three putative transmembrane domains and several MXM, MXXM, or MXXXM (where X is any other amino acid) methionine motifs (21). The long and short predicted peptides of CgCTR2 have two and three transmembrane domains, respectively, and each peptide contains four methionine motifs. These analyses suggested that Cg*CTR2* encodes a copper transporter of the vacuolar membrane.

**Functional complementation of *S. cerevisiae* CTR mutants.** Yeast *ctr* mutants were complemented with the Cg*CTR2* gene. The long and short Cg*CTR2* transcripts were expressed under the *GAL* promoter in an *S. cerevisiae ctr1*Δ *ctr2*Δ *ctr3*Δ triple mutant, which lacks the high affinity (*CTR1* and *CTR3*) and vacuole (*CTR2*) copper transporter genes. The triple *ctr* yeast mutant is unable to grow on ethanol-glycerol (YPEG) medium unless supplemented with >15 μM copper, unlike the *ctr1*Δ *ctr3*Δ double mutant, which can grow normally on YPEG medium with 15 μM copper (23). Expression of Cg*CTR2* in the *S. cerevisiae ctr1*Δ *ctr2*Δ *ctr3*Δ mutant strain fully restored growth on YPEG medium with 15 μM $CuCl_2$ (Fig. 3), further suggesting that CgCTR2 is a functional homologue of the *S. cerevisiae* Ctr2 vacuolar copper transporter.

**Cg*CTR2* localization.** To determine the localization of the Cg*CTR2* protein, we generated transgenic isolates expressing a CgCTR2-CFP fusion transcript. The cyan signal originating from the fusion protein was detected inside the cells, either as clear circles or as spots (Fig. 4). No signal could be detected on the outer cell membrane, suggesting that CgCTR2 is strictly localized inside the cell. Staining with the vacuole membrane-specific marker MDY-64 gave a similar staining pattern (Fig. 4A, frame c). Dual staining with both CFP and MDY-64 was not possible due to the overlapping of the excitation and emission spectra. In order to rule out possibility that the CFP was localized in nuclei, we compared Hoechst-stained nuclei with differential interference contrast (DIC) images (Fig. 4B). Vacuoles are clearly seen in the DIC images, and the overlay shows that nuclei are located between these large vacuoles. Although CFP signal surrounded the nuclei (open circles in Fig. 4A, frame a, and C, frames c and h), most of the CFP signal was detected inside large vacuoles or on the membranes of small vacuoles (Fig. 4C). Staining CgCRT2-CFP transgenic hyphae for a short period of time with FM4-64, which stained the cell plasma membrane, confirmed that the CFP signal was not localized in the cell plasma membrane (Fig. 4D, frames a and b). Staining for a longer period with FM4-64 resulted in FM4-64-labeled intracellular membranes that colocalized with the CFP signal (Fig. 4D, frames c, d, and e). These results chow that CgCTR2 is localized inside the cell in vacuoles and on vacuole membranes.

**Cg*CTR2* gene expression.** Expression of Cg*CTR2* was determined under various culture conditions, during germination, and following plant inoculation.

**Copper.** Response to copper was determined by exposing mycelia to 0, 10, 20, 100, and 250 μM concentrations of $CuCl_2$. Expression of CgCTR2 was highest on a medium without copper and slightly reduced by 10 and 20 μM $CuCl_2$. No further changes were observed at higher copper concentrations (Fig. 5A).

**Media.** To determine the effect of different media on CgCTR2 gene expression, we compared expression of CgCTR2 in mycelia that were produced in REG medium (a high osmotic, rich medium) and in PE or EMS medium, which induce pathogenic and saprophytic germination, respectively (3). Strongest expression was detected in spores and mycelia that were produced in REG (mycelium) and EMS (spores and mycelium) media whereas in PE medium the signal was below the detection level (Fig. 5B). These results are in agreement with the GFP expression pattern in strain N159, which was most intense in REG medium and in spores and hardly detected in PE medium (Fig. 1). To rule out the possibility that downregula-

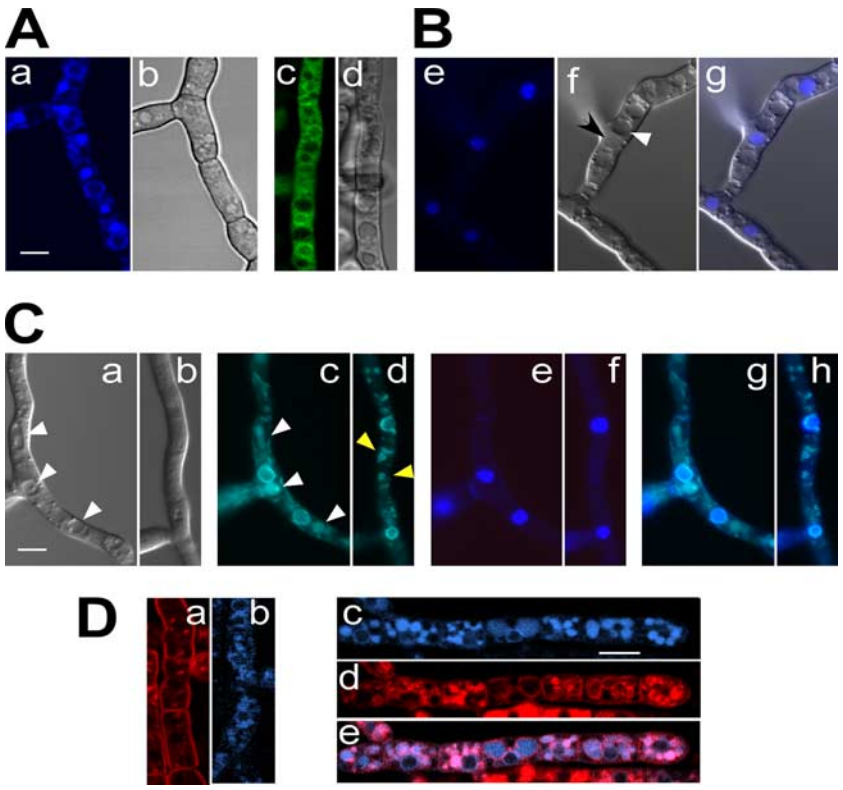


FIG. 4. CgCTR2 is localized in the vacuole membrane. Transformants expressing a CgCTR2-CFP fusion protein were visualized using confocal and fluorescent microscopes. (A) Confocal images of CFP and DMY-64 signals. Different samples are shown due to the overlap of the spectra between CFP and DMY-64. Frames a and b, CFP and DIC images; frames c and d, DMY-64 and DIC images. (B) Fluorescent microscopy of Hoechst-stained nuclei and DIC images. Frame e, Hoechst staining; frame f, DIC image (white arrow, vacuole; black arrow, nucleus); frame g, merge. (C) Fluorescent microscope images of CFP and Hoechst staining. Hyphae containing large (left) or small (right) vacuoles are shown. Frames a and b, DIC images; frames c and d, CFP (white arrows show large vacuoles; yellow arrows show small vacuoles); frames e and f, Hoechst staining; frames g and h, merged images of CFP and Hoechst staining. (D) Confocal images of FM4-64 and CFP signals. Frames a and b show the results of a short incubation with FM4-64. The FM4-64 signal (a) is detected on the outer cell membrane; CFP signal (b) is inside the cell; Frames c, d, and e show results of longer incubations with FM4-64: frame c, CFP; frame d, FM4-64; frame e, merged image. Membranes of large vacuoles are stained with FM4-64; CFP signal is localized inside these vacuoles as well as around nuclei. Scale bar, is 5 μm.

tion of the gene was possibly due to high copper levels in PE medium, we grew the N159 strain in PE medium supplemented with 5 and 100 μM copper or with the copper chelator EGTA. Under all of these conditions, expression of GFP was not altered and remained extremely low, indicating that the gene was repressed by components of the PE medium (data not shown).

**Germination.** Cg*CTR2* gene expression was followed in spores germinated in PE or EMS medium. In resting spores, expression of Cg*CTR2* was strong, similar to the GFP signal observed in spores produced by N159 on EMS plates. In EMS medium expression was stable throughout the entire germination process, whereas in PE medium Cg*CTR2* was downregulated already after 0.5 h, and no transcript could be detected thereafter (Fig. 5C).

**In planta.** Pea leaves were inoculated with spores, and tissue samples were collected from the infected area at several time points following inoculation. RNA was extracted from the infected plant tissues, and the relative expression of Cg*CTR2* was determined by quantitative RT-PCR. Expression of Cg*CTR2* was most intense in spores at time zero and was reduced to below detection levels immediately following plant inoculation, with no transcript detectable until 48 h postinoculation (Fig. 5D). A moderate level of Cg*CTR2* gene expression was recovered 72 h postinoculation.

The apparent expression pattern of Cg*CTR2* indicates that it is highly expressed in resting spores and strongly repressed at the onset of pathogenic development.

**Generation of CgCTR2 transgenic strains.** Insertion of the transformation cassette in strain N159 was at the 5′ untranslated region, close to the ATG, leaving the reading frame intact. RT-PCR analysis showed that Cg*CTR2* transcript levels were significantly reduced in strain N159 but not completely abolished (Fig. 6A). We used RNA interference (RNAi) to cause silencing of Cg*CTR2*. Complete silencing of Cg*CTR2* was obtained in RNAi strains 9 and 49 (Fig. 6A). Cg*CTR2*-overexpressing isolates were produced by expression of the gene from the *Aspergillus nidulans GPDA* promoter. Cg*CTR2* expression in these isolates was high under all conditions, including in PE medium, in which the Cg*CTR2* transcript is normally undetected (Fig. 6B). The N159 mutant strain was also transformed with a Cg*CTR2* complementation vector containing the Cg*CTR2* promoter and ORF. Analyses were car-

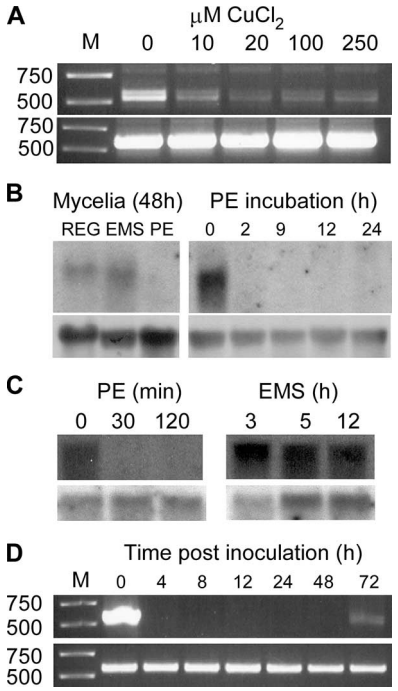


FIG. 5. Analysis of Cg*CTR2* gene expression. (A) Copper effect. Mycelium was collected after growth in REG medium for 44 h and incubated in medium containing various amounts of copper. After 4 h RNA was extracted, and cDNA was produced. RT-PCR was performed on the cDNA with Cg*CTR2*-specific primers, and samples were removed every 5 cycles starting at 15 cycles and up to 40 cycles. Picture shows samples collected after 35 cycles. Top, Cg*CTR2*; bottom, Cg*CDC42*. (B) Expression of Cg*CTR2* in different media and during pathogenic germination. Mycelium was grown for 48 h in different media, and then RNA was extracted, and transcript was detected by Northern blot analysis (left). Spores were collected from EMS plates and incubated in PE medium, which induces pathogenic germination (right). RNA was extracted at several time points starting at 2 h, which represents the onset of germ tube formation. Top, Cg*CTR2*; bottom, rRNA. (C) Expression during early stages of pathogenic and saprophytic germination. Spores were collected from plates and incubated in PE or EMS shake cultures. (D) In planta Cg*CTR2* gene expression. Pea leaves were inoculated with fresh spores, and tissue samples were collected at time intervals beginning at 4 h and up to 72 h postinoculation. Quantitative PCR was performed as described in panel A. Shown are results after 40 cycles. Top, Cg*CTR2*, bottom, Cg*CDC42*. Lanes M, molecular weight ladders.

ried out with complementation strains C10 and C37, which expressed normal levels of Cg*CTR2* (data not shown).

**Sensitivity of the Cg*CTR2* strains to copper and hydrogen peroxide.** Sensitivity to copper and oxidative conditions was determined by measuring the effect of $CuCl_2$ and hydrogen peroxide ($H_2O_2$) on radial growth. The addition of copper to the medium had the same effect on the growth rates of the wild-type and the transgenic strains; concentrations of 1 mM $CuCl_2$ or higher were lethal to all strains, whereas at lower copper concentrations the mutant and Cg*CTR2* overexpression strains had the same growth rates as the wild type (data not shown). The N159 and RNAi mutant strains were hypersensitive to $H_2O_2$, while the Cg*CTR2* overexpression strains were less sensitive and had a faster growth rate when grown on $H_2O_2$ than the wild-type 3.1.3 or Cg*CTR2* complementation strains (Table 2). These results are similar to those obtained in

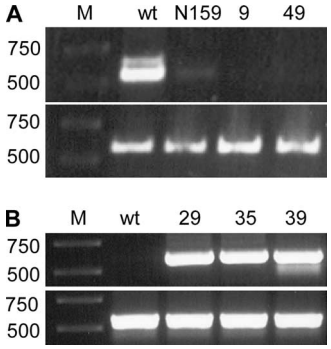


FIG. 6. Analysis of Cg*CTR2*-silenced and overexpression transgenic strains. (A) N159 and transgenic strains transformed with the Cg*CTR2* RNAi cassette (49 or 9). Strains were grown for 48 h in REG medium, conditions under which Cg*CTR2* gene expression is relatively strong. (B) Cg*CTR2*-overexpressing isolates. Strains were grown for 48 h in PE medium, conditions under which Cg*CTR2* gene expression is low. RNA was extracted, and RT-PCR was performed with primers specific for Cg*CTR2* (upper panel) and Cg*CDC42* (lower panel). Lanes M, molecular weight ladders; wt, wild type.

several yeast species in which *ctr2* mutants are unaffected in growth in response to copper but are hypersensitive to $H_2O_2$ (5, 16). In order to determine whether the hypersensitivity of the mutants to $H_2O_2$ was due to copper deficiency, we compared the growth rates of the strains on $H_2O_2$-containing medium supplemented with copper. The addition of low levels of copper (5 to 50 nM) had no effect on the growth rate of the wild type in $H_2O_2$-containing medium, but the same concentrations of copper greatly improved the growth rates of the mutants and restored the rates to wild-type levels (Table 3). The addition of iron instead of copper had no effect on the wild type or the mutants (data not shown). Thus, the hypersensitivity of Cg*ctr2* mutants to $H_2O_2$ can be specifically restored by an external supply of copper.

**Cu/Zn SOD activity in Cg*ctr2* mutants.** To test the postulated role of CgCTR2 in transporting copper to cytosolic copper-dependent enzymes, we measured the activity of the cytosolic Cu/Zn SOD enzyme, which requires copper for activity. Wild type and the RNAi 7 and N-159 mutant strains were grown in CD medium which does not contain copper. Mycelium was harvested after 48 h, and SOD activity was determined. Without copper, the wild type had an extra band that could not be detected in the mutants (Fig. 7). This band was intensified and was also detected in the mutants when copper

TABLE 2. Sensitivity of Cg*CTR2* transgenic strains to $H_2O_2$

| Strain | Radial growth (cm) at the indicated $H_2O_2$ concn (mM)[a] | | |
|---|---|---|---|
| | 0 | 3.2 | 4.8 |
| 3.1.3 (wild type) | 2.62 | 1.0 | 0.50 |
| N159 | 2.44 | 0.48 | 0.00 |
| RNAi 9 | 2.59 | 0.48 | 0.00 |
| OX29[b] | 2.59 | 1.42 | 0.94 |
| C10[c] | 2.60 | 0.92 | 0.45 |

[a] Values were determined after 5 days of incubation under dark conditions. Results are the means of four replications. The standard deviation was <0.1.
[b] OX29 is a Cg*CTR2* overexpression strain.
[c] C10 is a Cg*CTR2* complementation strain.

TABLE 3. Copper compensation for hypersensitivity of the Cg*ctr2* mutant to $H_2O_2$

| $CuCl_2$ concn (nM) | Radial growth (cm) of the indicated strain[a] | | | |
|---|---|---|---|---|
| | Without $H_2O_2$ | | With $H_2O_2$ (1.6 mM) | |
| | Wild type | Cg*ctr2* mutant | Wild type | Cg*ctr2* mutant |
| 0 | 2.20 ± 0.05 | 2.11 ± 0.03 | 0.80 ± 0.05 | 0.38 ± 0.07 |
| 5 | 2.11 ± 0.02 | 2.11 ± 0.02 | 0.77 ± 0.03 | 0.93 ± 0.03 |
| 25 | 2.15 ± 0.05 | 2.11 ± 0.03 | 0.76 ± 0.01 | 0.97 ± 0.05 |
| 50 | 2.11 ± 0.02 | 2.06 ± 0.02 | 0.75 ± 0.07 | 1.10 ± 0.03 |
| 500 | 2.07 ± 0.05 | 2.06 ± 0.03 | 0.75 ± 0.02 | 0.78 ± 0.05 |

[a] Growth was determined after 5 days of incubation under dark conditions. Values are the means of four replications ± standard deviations.

was added. These results show that under copper-limiting conditions, CgCTR2 is essential for supplying the copper required for the activity of a copper-dependent cytosolic enzyme. Two additional SOD activity bands, which were unaffected by copper, were observed under all conditions. These could be associated with Mn SOD.

**Spore germination in Cg*ctr2* mutants.** Spores ($10^6$/ml) of the RNAi strains had a reduced ability to germinate, similar to germination of N159 (Table 1). The germination defects of the Cg*ctr2* mutants were more pronounced at high spore densities. Less than 50% of Cg*ctr2* mutant conidia germinated at $2 \times 10^6$ or $10^6$ spores/ml, while at lower spore densities germination rates were increased and reached nearly wild-type levels at or below $10^5$ spores/ml (Fig. 8). Germination in the Cg*CTR2* overexpression and complementation strains was unchanged compared to the 3.1.3 wild-type strain (Table 1). Copper enhanced spore germination in both the Cg*ctr2* mutants and the wild-type strain. For the wild-type and N159 strains the germination rates in PE medium alone were 74% ± 3% and 39% ± 4%, respectively. With the addition of copper (100 μM $CuCl_2$), the germination rates were 87.6% ± 2% for the wild type and 54.8% ± 5% for strain N159. Thus, an external copper supply can enhance germination, but this phenomenon is unrelated to CgCTR2.

**Pathogenicity of the Cg*ctr2* mutants.** When sprayed ($5 \times 10^4$ spores/ml) on *A. virginica* plants, the Cg*ctr2* mutant strains (N159, RNAi 9, and RNAi 49) caused delayed and reduced symptoms compared with plants infected by the 3.1.3 wild-type

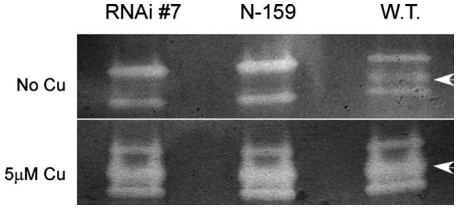


FIG. 7. Activity assay of Cu/Zn SOD in wild-type and Cg*ctr2* mutant strains. Strains were grown in CD medium without copper for 48 h. Mycelium was harvested, and SOD activity was determined with or without the addition of 5 μM copper. Without copper the wild type showed an additional band (arrow) that could not be detected in the RNAi and N159 mutant strains. This band was intensified and was present in all strains following the addition of 5 μM copper. The other two bands were unchanged under all conditions and might represent the activity of Mn SOD. WT, wild type.

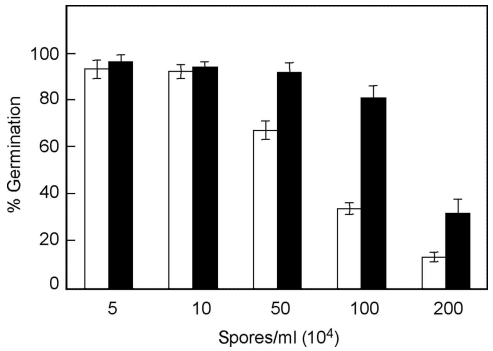


FIG. 8. Effect of spore density on germination rate. Spores of the wild-type (■) and N159 (□) strains were collected from EMS plates, diluted, and germinated in PE medium. After 2.5 h the number of germinated spores was counted, and the percentage of germination was calculated. Germination in the mutant strains was markedly reduced compared to the wild type at spore densities of $10^6$/ml or higher but was similar to the wild type at or below $10^5$ spores/ml.

strain. The level of plant mortality 6 days postinoculation was always lower than 50% in mutant-infected plants, compared to nearly 100% mortality in wild-type-infected plants (Fig. 9A). The complementation and overexpression strains had wild-type pathogenicity.

An onion epidermis penetration assay and inoculation of detached pea leaves were used to characterize the early stages of infection by the mutants. Since the RNAi and N159 strains had similar phenotypes, we used only the N159 strain in these experiments because it carried the GFP marker suitable for detection of in planta growth. There was no difference between N159 and the gGFP strain in appressorium formation and penetration on onion epidermis. In vitro assays of appressorium formation on petri dishes confirmed that the N159 strain was unaffected in appressorium formation (data not shown). Detached pea leaves developed similar symptoms when infected with spores of N159 or the GFP-expressing strains having wild-type pathogenicity, further demonstrating that the Cg*ctr2* mutants form fully functional appressoria (Fig. 9B). Thus, the Cg*CTR2* gene is dispensable for appressorium formation and function.

Usually, the fungus will penetrate the plant several hours after appressorium formation, and further development will occur inside the plant tissues (3, 4). Extensive hyphal growth on the plant surface was not observed in the wild-type strain 24 h postinoculation. In contrast, spores of strain N159 produced abundant hyphae on the leaf surface (Fig. 9B). The development of hyphae on the leaf surface has been previously correlated with saprophytic germination, in which germ tubes develop into long hyphae that do not differentiate appressoria (3).

Infection of *A. virginica* plants by *C. gloeosporioides* increases with increasing numbers of spores and reaches saturation at or near $5 \times 10^4$ spores/ml. Higher numbers of spores do not cause a significant increase in disease symptoms or plant mortality. The Cg*ctr2* mutants developed fully functional appressoria but had lower rates of pathogenic germination, which might affect the number of spores that can initiate infection. To determine whether low rates of pathogenic germination might cause the reduced virulence of Cg*ctr2* mutants, we compared disease

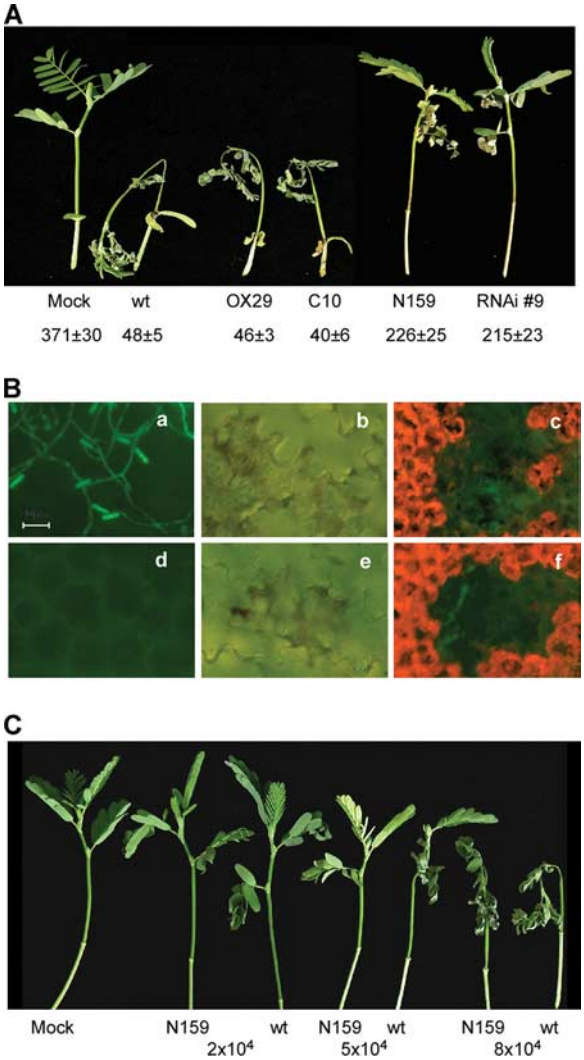


FIG. 9. Pathogenicity of Cg*ctr2* mutant strains. (A) Comparison of infection by the Cg*CTR2*-silenced and overexpression transgenic strains. *A. virginica* plants were inoculated with spore suspensions ($5 \times 10^4$ spores/ml) of wild type, N159, RNAi strains 9 and 49 (only strain 9 is shown), overexpression (OX) strains 29 and 35 (only strain OX29 is shown), and the N159 complemented strain C10. The picture shows plants at 6 days postinoculation. Numbers indicate the average fresh weight of six plants ± standard error. (B) Pea leaves were inoculated with spores of strain N159 (frames a to c) or with a GFP-expressing strain (frames d to f). After 24 h there is almost no external growth by the GFP-expressing strain (frame d), while N159 develops a significant amount of mycelium on the leaf surface (frame a). Leaves infected by strain N159 (frames b and c) develop necroses after 48 h, which are similar in size and number to the necroses that develop in leaves infected by the GFP-expressing strain (frames e and f). Images in frames a and d are from a light microscope; images in frames b to f are from a fluorescent stereoscope. (C) *A. virginica* plants were inoculated with optimal ($5 \times 10^4$), suboptimal ($2 \times 10^4$), and supraoptimal ($8 \times 10^4$) spore densities. Disease was recorded after 6 days. Full symptoms were developed by the inoculation of plants with $8 \times 10^4$ spores/ml of strain N159. All the experiments were repeated several times with similar results. wt, wild type.

levels at high ($8 \times 10^4$) or low ($2 \times 10^4$) numbers of spores with disease levels caused by $5 \times 10^4$ spores/ml. When plants were inoculated with $8 \times 10^4$ spores/ml, the symptoms caused by the Cg*ctr2* mutant strains were enhanced compared to infection with $5 \times 10^4$ spores/ml and were similar to symptoms caused by the 3.1.3 wild-type strain (Fig. 9C). When the number of spores was reduced to $2 \times 10^4$/ml, infection rates of both the wild type and N159 were reduced in comparison to infection with $5 \times 10^4$ spores/ml. The symptoms caused by $2 \times 10^4$ spores/ml of the wild-type strain were similar to the symptoms that were caused by $5 \times 10^4$ spores/ml of strain N159. That the reduced virulence of the Cg*ctr2* mutants could be compensated for by increasing the number of spores suggests that the low rates of spore germination among the mutants might contribute to their reduced virulence.

**The Mg*CTR2* gene in *M. grisea* is a functional homolog of Cg*CTR2*.** A single homolog of Cg*CTR2*, MGF00548, was identified in the *M. grisea* genome (named Mg*CTR2*). Three transformants of strain N159 carrying the Mg*CTR2* gene (entire ORF plus its native promoter) were generated and confirmed by Southern analysis (data not shown). Germination in N159::Mg*CTR2* strains was between 70% and 75%, significantly higher than 47% germination in N159 but somewhat lower than the 83% germination in the *C. gloeosporioides* wild-type strain 3.1.3 (Table 4). The hypersensitivity of Cg*ctr2* mutants to $H_2O_2$ was fully rescued by Mg*CTR2* (Table 4), indicating that Mg*CTR2* functionally complemented the *C. gloeosporioides* Cg*ctr2* mutant. Partial restoration of the germination defects in N159::Mg*CTR2* transformants might be related to the expression level of the Mg*CTR2* promoter in *C. gloeosporioides*.

To determine the function of Mg*CTR2* in *M. grisea*, we generated an Mg*ctr2* deletion mutant (see Materials and Methods). When assayed by vegetative growth on agar plates, the Mg*ctr2* mutant (strain CTR-23) showed increased sensitivity to $H_2O_2$ in comparison with the ectopic (CTR-18) transformant (Table 5). Spore germination was less sensitive to $H_2O_2$ than mycelium growth in the Mg*ctr2* mutant (Table 5). However, appressorium formation and melanization were highly sensitive to oxidative stress. As low as 0.8 mM $H_2O_2$ was effective in reducing appressorium formation, and no appressorium formation was observed in the Mg*ctr2* mutant in the presence of 3.2 mM $H_2O_2$. The increased sensitivity of the Mg*ctr2* mutant to oxidative stress further confirmed our earlier observations with the RNAi silencing transformants in *C. gloeosporioides* and showed that the function of Mg*CTR2* in *M. grisea* was similar to that of Cg*CTR2* in *C. gloeosporioides*.

TABLE 4. Germination rate and $H_2O_2$ sensitivity of N159::Mg*CTR2* strains

| Strain[a] | % Germination[b] | Radial growth (cm) at the indicated $H_2O_2$ concn (mM)[c] | | |
|---|---|---|---|---|
| | | 0 | 3.2 | 4.8 |
| 3.1.3 | 83 ± 4.0 | 1.87 | 0.51 | 0.30 |
| N159 | 47.8 ± 3.7 | 1.83 | 0.00 | 0.00 |
| MgCTR2-1 | 70.5 ± 4.8 | 1.90 | 0.53 | 0.00 |
| MgCTR2-3 | 69 ± 5.1 | 1.80 | 0.50 | 0.00 |

[a] MgCTR2-1 and MgCTR2-3: strain N159 complemented with *M. grisea* Mg*CTR2*, isolates 1 and 3, respectively. Similar results were obtained with additional isolates.

[b] Values are the means of four replications ± standard errors. All standard errors were <0.05.

[c] Growth was determined after 5 days of incubation under dark conditions.

TABLE 5. $H_2O_2$ sensitivity of Mg*ctr2* mutants[a]

| $H_2O_2$ concn (mM) | Growth (cm) | | % Germination | | % Appressorium formation | |
|---|---|---|---|---|---|---|
| | CTR-18 | CTR-23 | CTR-18 | CTR-23 | CTR-18 | CTR-23 |
| 0 | 4.0 ± 0.2 | 4.0 ± 0.2 | | | | |
| 0.8 | 3.8 ± 0.1 | 3.6 ± 0.1 | 96.1 ± 6.3 | 95.2 ± 7.3 | 87.2 ± 5.9 | 69.3 ± 6.9 |
| 1.6 | 3.5 ± 0.2 | 3.4 ± 0.1 | 95.2 ± 8.1 | 93.1 ± 8.9 | 72.1 ± 8.3 | 50.6 ± 5.9 |
| 3.2 | 3.0 ± 0.1 | 2.7 ± 0.1 | 92.3 ± 7.8 | 86.3 ± 9.3 | 51.6 ± 6.8 | |
| 6.25 | 1.6 ± 0.1 | | 87.8 ± 9.1 | 55.3 ± 7.2 | | |
| 12.5 | | | 63.9 ± 6.7 | 12.9 ± 2.2 | | |

[a] CTR-18, ectopic transformant; CTR-23, Mg*ctr2* deletion strain. Radial growth was determined after 5 days of incubation under dark conditions. Values are the means four replications ± standard errors.

## DISCUSSION

We previously showed that germination in *C. gloeosporioides* can follow two different routes, which are associated with pathogenic or saprophytic lifestyles (3). In the pathogenic mode, cell cycle and morphogenesis take place immediately after exposure to inducing signals, while in the saprophytic mode germination starts only several hours after induction. It is therefore suggested that pathogenic germination depends on genes (and proteins) that are expressed in the resting spores and can activate morphogenesis and the cell cycle upon receiving an appropriate signal. In this study, we exploited a collection of transgenic strains that were generated with a plasmid containing a *GFP* reporter gene to identify genes that are specifically related to pathogenic germination.

In strain N159, the GFP signal was intense in resting spores and was specifically repressed during pathogenic germination. The tagged locus was isolated, and the Cg*CTR2* gene, which is located 70 bp downstream of the insertion site in strain N159, was characterized. The predicted CgCTR2 protein shares high identity with *S. cerevisiae* Ctr2p, a copper transporter of the vacuolar membrane. The *S. cerevisiae* Ctr2p is a member of the CTR family of integral membrane proteins that function in copper uptake (1). The high-affinity copper transport protein members Ctr1p and Ctr3p are localized in the plasma membrane and import copper into the cell. These proteins have been studied in various organisms and are the primary transporters of external copper into the cell. A third member of the CTR family of proteins (Ctr2p) was studied in only a few species. It was initially identified by homology to the plant copper transporter Copt1 and was suggested to be a low-affinity copper transporter due to lack of a clear phenotype in yeast and *Podospora anserine ctr2*Δ mutants (6, 10). However, more recent studies showed that Ctr2p is localized to the vacuole membrane and that it is involved in regulation of the intracellular copper concentration by exporting copper from the vacuole into the cytosol (23). Localization of the *Arabidopsis* and *P. anserine* homologs is unknown, but they might well represent vacuolar transporters.

The redox sensitivity of copper makes it an essential cofactor in critical biological processes such as respiration, iron transport, oxidative stress protection, and pigmentation. *S. cerevisiae ctr1*Δ *ctr3*Δ *ctr2*Δ triple mutants are unable to grow on ethanol-glycerol medium (YPEG) due to insufficient delivery of copper to cytochrome *c* oxidase. The strain can grow only on YPEG medium containing relatively high levels of copper. This defect is partially compensated for by complementation of the triple *ctr*Δ mutant with the wild-type *CTR2* gene (23). *S. cerevisiae ctr1*Δ *ctr3*Δ *ctr2*Δ expressing Cg*CTR2* (either the long or short transcript) was unable to grow on YPEG medium without copper but exhibited improved growth on YPEG medium with a low copper concentration, which was even better than the growth of the same strain complemented with *S. cerevisiae CTR2* (Fig. 3). Further, a CgCTR2-CFP fusion protein was localized in vacuoles (Fig. 4), similar to yeast Ctr2p (23). In large vacuoles the signal was detected inside the vacuoles, whereas in small vacuoles it was detected on the vacuole membrane. The localization inside large vacuoles could be the result of the overexpression or be due to the internalization of the protein following inactivation of these vacuoles. Importantly, CgCTR2 could not be detected in the cell plasma membrane, thus ruling out the possibility that this protein is similar to CTR1 or CTR3 and involved in copper uptake. Together, the sequence homology, functional analysis, and localization data strongly suggest that CgCTR2 is a vacuole copper transporter.

Yeast *CTR2* encodes a single peptide, whereas the Cg*CTR2* produces two transcripts, which result from an alternative splicing of the coding sequence. CTR proteins contain three putative transmembrane regions and an amino-terminal region that is rich in methionine motifs (22). Two or three transmembrane domains were found in the long and short polypeptides of CgCTR2, respectively, which are situated in the middle and at the carboxy terminus of the protein. This configuration is highly similar to the transmembrane domains found in *C. albicans* Ctr1p (16). The shorter transcript was more abundant in RNA samples obtained from fungal cultures and from fungus-infected plants (Fig. 5A and 6A and D), which could suggest different roles of the two peptides. However, both transcripts were fully functional in yeast (Fig. 3), and when overexpressed in *C. gloeosporioides*, the large transcript was predominant (Fig. 6B). Therefore, the functional significance of the alternative splicing of Cg*CTR2* remains unclear.

Complementation of strain N159 with an intact copy of Cg*CTR2* fully restored the wild-type phenotype, confirming that the observed phenotypes of the N159 and RNAi strains resulted from reduced Cg*CTR2* expression. The *M. grisea CTR2* homolog Mg*CTR2* also complemented strain N159 although germination was not fully restored, possibly because the Mg*CTR2* gene was expressed from its own promoter. Exchanging the tightly regulated promoters between these fungi resulted in different expression patterns (14) and therefore

might not be as efficient as expressing the gene from the native promoter.

Dormant spores contain various transcripts, some of which disappear soon after spore germination. These genes might be needed for activation of growth in dormant spores upon receiving the right signals (17). Cg*CTR2* was highly expressed in resting spores, and the transcript and protein quickly disappeared during pathogenic germination, suggesting that Cg*CTR2* may be required for the activation of pathogenic germination, which represents the onset of pathogenic development. One explanation for the specific effect of the Cg*CTR2* silencing on only pathogenic germination would be that copper-requiring enzymes that are involved in activation of the initial stages of pathogenic germination depend on an intracellular copper supply. The high-level expression of Cg*CTR2* in resting spores indicates that supplying copper to cytoplasmic enzymes does not depend on de novo synthesis of proteins and can take place without any delay at the onset of germination by transport of copper from the vacuole. Indeed, addition of copper to the medium did not overcome the germination defects of Cg*ctr2* mutants, but it caused a 15% increase in germination of the wild type as well as mutant spores, further demonstrating that copper is necessary for the early stages of germination.

The role of copper in the early stages of fungal pathogenesis is supported by microarray data derived from in planta experiments, in which a number of copper-related genes are found among fungal transcripts that are differentially upregulated (9, 20, 28). We also found a high frequency of expressed sequence tags of several copper-related genes in a cDNA library prepared from pathogenic, germinated spores, including the Ctr3p and Ctr2p copper transporters, the copper chaperone TahA, Cu-transporting P1-type ATPase Crd1p, and a multicopper oxidase (S. Barhoom and A. Sharon, unpublished data). Deletion of a *Colletotrichum lindemuthianum* copper-transporting ATPase *CLAP1*, which is involved in intracellular delivery of copper to copper-requiring enzymes, resulted in mutants that were unable to induce disease symptoms, further demonstrating the importance of proper intracellular copper transport in fungal pathogenesis (18).

*C. gloeosporioides* and *M. grisea ctr2* mutant strains showed increased sensitivity to hydrogen peroxide, whereas overexpression of Cg*CTR2* increased resistance to oxidative stress. Due to its ability to adopt both oxidized and reduced states, copper is an important redox cofactor in many copper-dependent enzymes such as polyphenol oxidase, cytochrome *c* oxidase, and copper/zinc SOD (34). *C. albicans*, yeast, and human *ctr1*-null mutants also display increased sensitivity to hydrogen peroxide, which was explained by copper/zinc SOD defects (16, 22). In agreement with this possibility, we showed that low levels of copper (but not iron) reduced sensitivity of Cg*CTR2* mutants to hydrogen peroxide and reversed it to wild-type levels, whereas the same copper concentrations had no effect on the wild-type sensitivity to hydrogen peroxide (Table 3). These results demonstrate the importance of copper in oxidative stress resistance and the involvement of Cgctr2 in maintaining optimal levels of free copper in the cytoplasm.

Differences were found in the sensitivity of *C. gloeosporioides* and *M. greisea ctr2* mutants to oxidative stress at different stages of development, with appressorium formation being the most sensitive. The *C. lindemuthianum clap1* (copper-transporting ATPase) mutant is characterized by beige mycelium and appressoria instead of the normal black pigmentation of these organs (18). Addition of $CuSo_4$ restored the black pigmentation in *clp1* mycelium but not in the appressoria of the mutant, indicating that appressorium melanization might depend on internal copper translocation, which directs copper to the correct cellular compartments (18). In other organisms such as plants or yeasts, many genes are involved in copper uptake, distribution, and sequestration through copper-responsive transcription factors. Once the copper is inside the cell, $Cu^{+2}$ chaperones mediate intracellular copper delivery to specific targets such as the mitochondria, vacuole, chloroplast, and the secretory pathway (22, 24). The mechanism of communication between intracellular compartments and cuproproteins in the cytosol and the plasma membrane is still unknown, but CTR2 is probably an important player in this intracellular copper-distributing apparatus.

The Cg*ctr2* mutant strains had reduced pathogenicity. The difference from wild type was quantitative and could be compensated for by increasing the number of spores used for plant inoculation. No defects were found in appressorium formation or penetration in pea leaves and onion epidermis assays, and disease symptoms developed on the same time scale as in wild-type-infected leaves. These results suggest that the reduced pathogenicity of the Cg*ctr2* mutants might be a consequence of reduced levels of pathogenic germination rather than a direct defect in pathogenicity. However, other factors that have not yet been determined could be responsible for this phenotype.

Free sugars are sufficient to activate germination in many fungi. In a classical scenario, dormant spores are activated by, e.g., glucose and then undergo isotropic growth, which can last for several hours, before polarized growth and cell cycle are initiated. Spores of plant-pathogenic fungi germinate in a nutrient-depleted environment and therefore must respond to stimuli that come from their host plant. Because of the lack of an external nutritional source, spores of plant pathogens must rely on internal resources to quickly complete the developmental stages that are necessary for host penetration. Here, we showed that a vacuolar copper transporter that is highly expressed in resting spores (CgCTR2) is necessary for optimal germination. Previous works showed that many fungal copper metabolic genes are induced during pathogenesis, and proper copper translocation by the copper-transporting ATPase CLAP1 is essential for pathogenesis in *C. lindemuthianum* (18). Our results show that copper is needed at the initial stages of pathogenesis in *C. gloeosporioides* and that the putative vacuole copper transporter CgCTR2 is probably involved in this process.

## ACKNOWLEDGMENTS

We are grateful to Dennis J. Thiele for providing the yeast *ctr*Δ strains and plasmids.

This work was supported by grant US-3491-03 from BARD to A.S. and J.-R.X.

## REFERENCES

1. **Aller, S. G., E. T. Eng, C. J. De Feo, and V. M. Unger.** 2004. Eukaryotic CTR copper uptake transporters require two faces of the third transmembrane domain for helix packing, oligomerization, and function. J. Biol. Chem. **279:**53435–53441.

2. **Bagga, S., and D. Straney.** 2000. Modulation of cAMP and phosphodiesterase activity by avonoids which induce spore germination of *Nectria haematococca* MP VI (*Fusarium solani*). Physiol. Mol. Plant Pathol. **56:**51–61.
3. **Barhoom, S., and A. Sharon.** 2004. cAMP regulation of "pathogenic" and "saprophytic" fungal spore germination. Fungal Genet. Biol. **41:**317–326.
4. **Barhoom, S., and A. Sharon.** 2007. Bcl-2 proteins link programmed cell death with growth and morphogenetic adaptations in the fungal plant pathogen *Colletotrichum gloeosporioides*. Fungal Genet. Biol. **44:**32–43.
5. **Bellemare, D. R., L. Shaner, K. A. Morano, J. Beaudoin, R. Langlois, and S. Labbe.** 2002. Ctr6, a vacuolar membrane copper transporter in *Schizosaccharomyces pombe*. J. Biol. Chem. **277:**46676–46686.
6. **Borghouts, C., C. Q. Scheckhuber, O. Stephan, and H. D. Osiewacz.** 2002. Copper homeostasis and aging in the fungal model system *Podospora anserine*: differential expression of PaCTR3 encoding a copper transporter. International J. Biochem. Cell Biol. **34:**1355–1371.
7. **Chaky, J., K. Anderson, M. Moss, and L. Vaillancourt.** 2001. Surface hydrophobicity and surface rigidity induce spore germination in *Colletotrichum graminicola*. Phytopathology **91:**558–564.
8. **Doehlemann, G., P. Berndt, and M. Hahn.** 2006. Different signaling pathways involving a Gα protein, cAMP and a MAP kinase control germination of *Botrytis cinerea* conidia. Mol. Microbiol. **59:**821–835.
9. **Guldener, U., K. Y. Seong, J. Boddu, S. Cho, F. Trail, J. R. Xu, G. Adam, H. W. Mewes, G. J. Muehlbauer, and H. C. Kistter.** 2006. Development of a *Fusarium graminearum* Affymetrix GeneChip for profiling fungal gene expression in vitro and in planta. Fungal Genet. Biol. **43:**316–325.
10. **Kampfenkel, K., S. Kushnir, E. Babiychuk, D. Inze, and M. Van Montagu.** 1995. Molecular characterization of a putative *Arabidopsis thaliana* copper transporter and its yeast homologue. J. Biol. Chem. **270:**28479–28486.
11. **Kim, Y. K., D. Li, and P. E. Kolattukudy.** 1998. Induction of $Ca^{+2}$ calmodulin signaling by hard surface contact primes *Colletotrichum gloeosporioides* conidia to germinate and form appressoria. J. Bacteriol. **180:**5144–5150.
12. **Kolattukudy, P. E., L. M. Rogers, D. Li, C. S. Hwang, and M. A. Flaishman.** 1995. Surface signaling in pathogenesis. Proc. Natl. Acad. Sci. USA **92:**4080–4087.
13. **Lee, S. C., and Y. H. Lee.** 1998. Calcium/calmodulin-dependent signaling for appressorium formation in the plant pathogenic fungus *Magnaporthe grisea*. Mol. Cells **8:**698–704.
14. **Li, L., S. L. Ding, A. Sharon, and J. R. Xu.** 2007. A novel nuclear protein Mir1 is highly up-regulated during infectious hyphal growth in the rice blast fungus. Mol. Plant Microbe. Interact. **20:**448–458.
15. **Liu, Z. M., and P. E. Kolattukudy.** 1999. Early expression of the calmodulin gene, which precedes appressorium formation in *Magnaporthe grisea*, is inhibited by self-inhibitors and requires surface attachment. J. Bacteriol. **181:**3571–3577.
16. **Marvin, M. E., P. H. Williams, and A. M. Cashmore.** 2003. The *Candida albicans* CTR1 gene encodes a functional copper transporter. Micobiology **149:**1461–1474.
17. **Osherov, N., and G. S. May.** 2001. The molecular mechanisms of conidial germination. FEMS Microbiol. Lett. **199:**153–160.
18. **Parisot, D., M. Dufresne, C. Veneault, R. Lauge, and T. Langin.** 2002. *clap1*, a gene encoding a copper-transporting ATPase involved in the process of injection by the phytopathogenic fungus *Colletotrichum lindemuthianum*. Mol. Genet. Genomics **268:**139–151.
19. **Podila, G. K., L. M. Rogers, and P. E. Kolattukudy.** 1993. Chemical signals from avocado surface wax trigger germination and appressorium formation in *Colletotrichum gloeosporioides*. Plant Physiol. **103:**267–272.
20. **Posada-Buitrago, M. L., and R. D. Frederick.** 2005. Expressed sequence tag analysis of the soybean rust pathogen *Phakopsora pachyrhizi*. Fungal Genet. Biol. **42:**949–962.
21. **Puig, S., J. Lee, M. Lau, and D. J. Thiele.** 2002. Biochemical and genetic analyses of yeast and human high affinity copper transporters suggest a conserved mechanism for copper uptake. J. Biol. Chem. **277:**26021–26030.
22. **Puig, S., and D. J. Thiele.** 2002. Molecular mechanisms of copper uptake and distribution. Curr. Opin. Chem. Biol. **6:**171–180.
23. **Rees, E. M., J. Lee, and D. J. Thiele.** 2004. Mobilization of intracellular copper stores by the Ctr2 vacuolar copper transporter. J. Biol. Chem. **279:**54221–54229.
24. **Rees, E. M., and D. J. Thiele.** 2004. From aging to virulence: forging connections through the study to copper homeostasis in eukaryotic microorganisms. Curr. Opin. Microbiol. **7:**175–184.
25. **Robinson, M., J. Riov, and A. Sharon.** 1998. Indole-3-acetic acid biosynthesis in *Colletotrichum gloeosporioides* f. sp. *Aeschynomene*. Appl. Environ. Microbiol. **64:**5030–5032.
26. **Robinson, M., and A. Sharon.** 1999. Transformation of the bioherbicide *Colletotrichum gloeosporioides* f. sp. *aeschynomene* by electroporation of germinated conidia. Curr. Genet. **36:**98–104.
27. **Shaw, B. D., and H. C. Hoch.** 2000. $Ca^{+2}$ regulation of *Phyllosticta ampelicida* pycnidiospore germination and appressorium formation. Fungal Genet. Biol. **31:**43–53.
28. **Soanes, D., and N. J. Talbot.** 2005. A bioinformatic tool for analysis of EST transcript abundance during infection-related development by *Magnaporthe grisea*. Mol. Plant Pathol. **6:**503–512.
29. **Takano, Y., T. Kikuchi, Y. Kubo, J. E. Hamer, K. Mise, and I. Furusawa.** 2000. The *Colletotrichum lagenarium* MAP kinase gene *CMK1* regulates diverse aspects of fungal pathogenesis. Mol. Plant Microbe Interact. **13:**374–383.
30. **Takano, Y., W. Choi, T. K. Mitchell, T. Okuno, and R. A. Dean.** 2003. Large scale parallel analysis of gene expression during infection-related morphogenesis of *Magnaporthe grisea*. Mol. Plant Pathol. **4:**337–346.
31. **Xu, J. R.** 2000. MAP kinases in fungal pathogens. Fungal Genet. Biol. **31:**137–152.
32. **Xue, C., G. Park, W. Choi, L. Zheng, R. A. Dean, and J. R. Xu.** 2002. Two novel fungal virulence genes specifically expressed in appressoria of the rice blast fungus. Mol. Plant Microbe Interact. **15:**1119–1127.
33. **Zhao, X., Y. Kim, G. Park, and J. R. Xu.** 2005. A mitogen-activated protein kinase cascade regulating interaction related morphogenesis in *Magnaporthe grisea*. Plant Cell **17:**1317–1329.
34. **Zhou, H., and D. J. Thiele.** 2001. Identification of a novel high affinity copper transport complex in the fission yeast *Schizosaccharomyces pombe*. J. Biol. Chem. **276:**20529–20535.